PHYSICAL REVIEW D **82,** 014002 (2010)

# Impact of parton distribution function and $\alpha_s$ uncertainties on Higgs boson production in gluon fusion at hadron colliders

Federico Demartin,[1] Stefano Forte,[1,2] Elisa Mariani,[1] Juan Rojo,[2] and Alessandro Vicini[1,2]

[1]*Dipartimento di Fisica, Università di Milano, Via Celoria 16, I–20133 Milano, Italy*

[2]*INFN, Sezione di Milano, Via Celoria 16, I–20133 Milano, Italy*

(Received 9 April 2010; published 8 July 2010)

We present a systematic study of uncertainties due to parton distributions (PDFs) and the strong coupling on the gluon-fusion production cross section of the standard model Higgs at the Tevatron and LHC colliders. We compare procedures and results when three recent sets of PDFs are used, CTEQ6.6, MSTW08, and NNPDF1.2, and we discuss specifically the way PDF and strong coupling uncertainties are combined. We find that results obtained from different PDF sets are in reasonable agreement if a common value of the strong coupling is adopted. We show that the addition in quadrature of PDF and $\alpha_s$ uncertainties provides an adequate approximation to the full result with exact error propagation. We discuss a simple recipe to determine a conservative PDF + $\alpha_s$ uncertainty from available global parton sets, and we use it to estimate this uncertainty on the given process to be about 10% at the Tevatron and 5% at the LHC for a light Higgs.

DOI: 10.1103/PhysRevD.82.014002 PACS numbers: 12.38.−t, 13.85.Qk

## I. INTRODUCTION

At the dawn of experimentation of LHC it is important to assess carefully the expected accuracy of standard candle signal and background measurements. Standard model Higgs production is clearly one such process. The main production mechanism for a scalar Higgs boson at the LHC is the gluon-fusion process ($pp \to H + X$) [1]. This process is also an especially interesting test case to study QCD uncertainties: on the one hand, it starts at $O(\alpha_s^2)$ and it undergoes large $O(\alpha_s^3)$ corrections which almost double the cross section [2,3]. On the other hand, it is driven by the gluon distribution, which is only determined starting at $O(\alpha_s)$ (unlike quark distributions which can be determined from parton-model processes). Therefore, this process is quite sensitive both to parton distributions (PDFs) and $\alpha_s$ uncertainties, and also on their interplay.

Our knowledge of PDFs (see Refs. [4,5]) and of $\alpha_s$ (see Refs. [6,7]) have considerably improved in the last several years. However, they remain the main source of phenomenological uncertainty related to the treatment of the strong interaction: they limit the accuracy in a way which cannot be improved upon by increasing the theoretical accuracy. It is the purpose of this work to explore this uncertainty using Higgs production in gluon-fusion as a test case. Our goal is fivefold:

(i) We would like to compare the procedure recommended by various groups to combine PDF uncertainties and $\alpha_s$ uncertainties (and specifically Hessian-based approaches with Monte Carlo approaches) both in terms of procedure and in terms of results.

(ii) We would like to assess the impact of the correlation between the value of $\alpha_s$ and the PDFs both when determining central values and uncertainty bands, and specifically understand how much results change when this correlation is taken into account in comparison to the case in which $\alpha_s$ and PDF variations are done independently with results added in quadrature.

(iii) We would like to assess how much of the difference in results found when using different PDF sets (both for central values and uncertainty bands) is due to the PDFs, and how much is due to the choice of value of $\alpha_s$.

(iv) We would like to compare how much of the total uncertainty is due to $\alpha_s$ and how much is due to PDFs.

(v) We would like to arrive at an assessment of the value of this cross section as well as the PDF + $\alpha_s$ uncertainty on it, and more in general at a procedure to estimate them.

For each of these issues Higgs production through gluon-fusion is an interesting test case in that it is likely to provide a worst case scenario: differences between results obtained using different PDF sets or following different procedures for the combination of uncertainties are likely to be smaller for many other relevant processes. For instance, in processes involving quark PDFs the correlation between PDFs and the value of $\alpha_s$ is likely to be weaker, and thus the results found adding uncertainties in quadrature are likely to differ less from those obtained when the correlation between PDFs and $\alpha_s$ is fully accounted for.

The studies performed here will be done using PDF sets from the CTEQ, MSTW, and NNPDF Collaborations, specifically the PDF sets CTEQ6.6 [8], MSTW08 [9], and NNPDF1.2 [10,11]. In order to account for the $\alpha_s$ dependence, we will use PDF sets with varying $\alpha_s$ which have been published by CTEQ [8] and MSTW [12], as well as NNPDF1.2 sets with varying $\alpha_s$ [13] which will be presented here for the first time. Comparison between CTEQ and MSTW on one side and NNPDF on the other side will enable us to contrast results obtained in the Hessian approach of the former with those found in the Monte Carlo approach of the latter. Computations will be performed at next-to-leading order (NLO) in the strong coupling $\alpha_s$, because, even though NNLO results for the process we study are available [14], global parton fits with a full treatment of both DIS and hadronic data only exist at NLO (for instance, the MSTW08 set [9] only treats DIS fully at NNLO, while Drell-Yan is described using $K$-factors, and jets using NLO theory). There are of course several other sources of uncertainty on standard candles at colliders, such as electroweak uncertainties and further QCD uncertainties unrelated to PDFs, but their study goes beyond the scope of this work: here we concentrate on PDF uncertainties, and on the $\alpha_s$ uncertainty which is tangled with them.

The outline of the paper is as follows: in Sec. II we summarize the computation of the Higgs production cross section and the choice of value of $\alpha_s$. In Sec. III we discuss and compare PDF sets with varying $\alpha_s$, and specifically present the NNPDF1.2 sets with varying $\alpha_s$, which allow for a direct computation of the correlation between $\alpha_s$ and the gluon. We then turn to a comparison of predictions obtained using different PDF sets: first, in Sec. IV we study PDF uncertainties and compare predictions for the cross section and the PDF uncertainty on it obtained using different sets; then in Sec. V we discuss $\alpha_s$ uncertainties and their combination with PDF uncertainties; finally in Sec. VI we compare final results and discuss a procedure to construct a combined prediction from the available sets. Conclusions are drawn in Sec. VII.

## II. THE HIGGS BOSON PRODUCTION CROSS SECTION

### A. The hadron-level cross section

The hadronic total cross section for the production of a standard model Higgs of mass $m_H$ via gluon-fusion at center-of-mass energy $\sqrt{s}$ is

$$\sigma(h_1 + h_2 \to H + X) = \sum_{a,b} \int_0^1 dx_1 dx_2 f_{a,h_1}(x_1, \mu_F^2) \times f_{b,h_2}(x_2, \mu_F^2) \times \int_0^1 dz \delta\left(z - \frac{\tau_H}{x_1 x_2}\right) \hat{\sigma}_{ab}(z), \quad (1)$$

where $\tau_H = m_H^2/s$, $\mu_F$ is the factorization scale, $f_{a,h_i}(x, \mu_F^2)$ are the PDFs for parton $a$, ($a = g, q, \bar{q}$) of hadron $h_i$, and $\hat{\sigma}_{ab}$ is the cross section for the partonic subprocess $ab \to H + X$ at the center-of-mass energy $\hat{s} = x_1 x_2 s = m_H^2/z$. The latter can be written as

$$\hat{\sigma}_{ab}(z, \mu_R^2) = \sigma^{(0)}(\mu_R^2) z G_{ab}(z, \mu_R^2), \quad (2)$$

where the Born cross section is

$$\sigma^{(0)}(\mu_R^2) = \frac{G_\mu \alpha_s^2(\mu_R^2)}{512\sqrt{2}\pi} \left| \sum_q \mathcal{G}_q^{(1l)} \right|^2 \quad (3)$$

and the sum runs over all quark flavors that appear in the amplitude $\mathcal{G}^{(1l)}$, with

$$\mathcal{G}_q^{(1l)} = -4y_q[2 - (1 - 4y_q)H(0, 0, x_q)]. \quad (4)$$

In Eq. (4) we have defined

$$y_q \equiv \frac{m_q^2}{m_H^2}, \qquad x_q \equiv \frac{\sqrt{1 - 4y_q} - 1}{\sqrt{1 - 4y_q} + 1}, \qquad H(0, 0, z) = \frac{1}{2}\log^2(z), \quad (5)$$

with the standard notation for harmonic polylogarithms (HPLs).

Up to NLO,

$$G_{ab}(z) = G_{ab}^{(0)}(z) + \frac{\alpha_s(\mu_R^2)}{\pi} G_{ab}^{(1)}(z) \quad (6)$$

where $a$; $b$ stand for any allowed parton. Exact analytic results, with the full dependence on the masses of the quarks running in the loop, have been obtained for the NLO coefficient function $G_{ab}^{(1)}$ in [3] and more recently in terms of HPLs in [15].

All numerical results presented in this paper have been obtained using a code based on the expressions of Ref. [15]. We will consider only the gluon-gluon channel, and evaluate the total cross section at NLO-QCD, with the running of the strong coupling constant $\alpha_s(\mu_R^2)$ implemented as discussed in Sec. II B below. The default choice for the renormalization scale is $\mu_R = m_H$. The cross sections have been computed including the contributions due to the top and the bottom quark running in the fermion loop, with masses $m_t = 172$ GeV and $m_b = 4.6$ GeV; the value of the Fermi constant is $G_\mu = 1.166\,37 \times 10^5\ \mathrm{GeV}^{-2}$. The top mass has been renormalized in the on-shell scheme [3,15].

### B. The strong coupling $\alpha_s$

Even though the strong coupling $\alpha_s$ can be determined by a parton fit [12], its most accurate determination is arrived at by combining results from many high-energy processes, most of which do not depend on PDFs at all. A recent combined determination [7] is

$$\alpha_s(M_Z) = 0.1184 \pm 0.0007, \quad (7)$$

while the currently published[1] PDG average [6] has a rather more conservative assessment of the uncertainty:

[1]The 2009 web PDG update [16] no longer provides a combined determination of $\alpha_s$, and refers to Ref. [7].

$$\alpha_s(M_Z) = 0.1176 \pm 0.002. \quad (8)$$

Both these uncertainties should be understood as one-$\sigma$, i.e. 68% confidence levels.

Because it starts at order $\alpha_s^2$ and it undergoes sizable $O(\alpha_s^3)$ corrections, the Higgs cross section is very sensitive to the central value of the strong coupling and it is thus important to compare results obtained using the same value of $\alpha_s$. However, different values of $\alpha_s$ are adopted by various parton fitting groups. Specifically, for the PDF sets we are interested in, the reference values are

$$\begin{aligned} \alpha_s(M_Z) &= 0.118 \quad \text{for CTEQ6.6,} \\ \alpha_s(M_Z) &= 0.119 \quad \text{for NNPDF1.2,} \\ \alpha_s(M_Z) &= 0.12018 \quad \text{for MSTW08.} \end{aligned} \quad (9)$$

Therefore, in order to obtain a meaningful comparison, we must study the dependence of results obtained with different sets when the value of $\alpha_s$ is varied about the central values of Eq. (9).

For comparison of relative uncertainties, which are less sensitive to central value of $\alpha_s$, but of course very sensitive to the range in which $\alpha_s$ is varied, we will assume that the one-$\sigma$ and 90% confidence level variations of $\alpha_s$ are, respectively, given by

$$\Delta^{(68)}\alpha_s = 0.0012 = 0.002/c_{90} \quad (10)$$

$$\Delta^{(90)}\alpha_s = 0.002, \quad (11)$$

where $c_{90} = 1.644\,85\ldots$ is the number of standard deviations for a Gaussian distribution that corresponds to a 90% C.L. interval. Our choice Eqs. (10) and (11) is thus intermediate between the choices in Eqs. (8) and (7). A reassessment of the value $\alpha_s$ and its uncertainty go beyond the scope of this work: these values are chosen as a reasonable reference, and ensure that our results will also be valid for other reasonable choices in the same ballpark.

An important subtlety is the number of active flavours in the running of the strong coupling, as implemented by various PDF analyses. Indeed, QCD calculations are usually performed in a decoupling scheme [17], in which heavy flavors decouple at scales much lower than their mass. When studying a process like Higgs production for a wide range of the Higgs mass one must then specify what to do above top threshold, and specifically fix the scale at which heavy quarks decouple, which amounts to a choice of renormalization scheme. This choice should be used consistently in the running of $\alpha_s$, the evolution equations for PDFs, and the computation of hard matrix elements. In Refs. [3,15], a scheme in which the number of active flavours becomes $n_f = 6$ at $Q^2 = m_t^2$ is adopted; this scheme is also used by NNPDF. However, CTEQ and MSTW instead use a scheme in which $n_f = 5$ even when $Q^2 > m_t^2$ both in the running of the strong coupling and in PDF evolution.

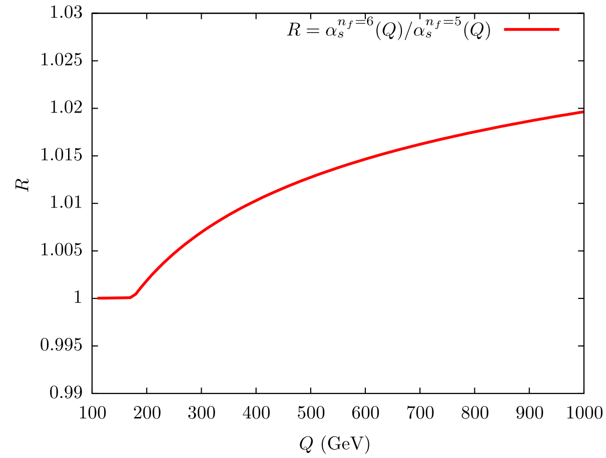


FIG. 1 (color online). Ratio of the strong coupling determined with a number of flavors that varies from $n_f = 5$ to $n_f = 6$ at $Q > m_t$ to that with $n_f = 5$ at all scales.

The effect of this on the running of $\alpha_s$ is small but nonnegligible: in Fig. 1 we plot the ratio of the variable-flavor $\alpha_s$ to the fixed-flavor one, and show that for $Q = 2m_t$ the discrepancy is already of order of 1%, and thus the effect on a quantity which depends on higher powers of $\alpha_s$ accordingly larger. Of course, this scheme dependence cancels to a large extent once PDFs and hard cross sections are consistently combined, and a fully consistent comparison would require the use of the same scheme everywhere. This is difficult in practice because of the different choices adopted by NNPDF on the one hand, and CTEQ and MSTW on the other hand. For the sake of comparisons below, we will use the NLO Higgs cross section from Refs. [3,15] and, consistently $\alpha_s$ which runs with $n_f$ that varies at $Q = m_t$: this is then also consistent with the evolution equations used to construct the NNPDF set, but not with those used to construct the CTEQ and MSTW set. It should be borne in mind that this incomplete cancellation of the scheme dependence above the top threshold may lead to a spurious difference between central values at the percent level between NNPDF and other groups.

## III. PARTON SETS WITH VARIABLE STRONG COUPLING

### A. PDFs and $\alpha_s$ in a Hessian approach

PDF sets with varying $\alpha_s$ have been presented by the CTEQ [8] and MSTW [12] collaborations. Specifically, CTEQ has released the CTEQ6.6alphas sets, which add to the central CTEQ6.6 fit [8], which has $\alpha_s = 0.118$, four more sets with $\alpha_s = 0.116$, 0.117, 0.119, 0.120. In these fits, $\alpha_s$ is taken as an external parameter which is fixed each time to the given value along with all other physical parameters in the fit (such as, say, the fine-structure constant or the $W$ mass). However, eigenvector PDF sets for the computation of PDF uncertainties are only provided for

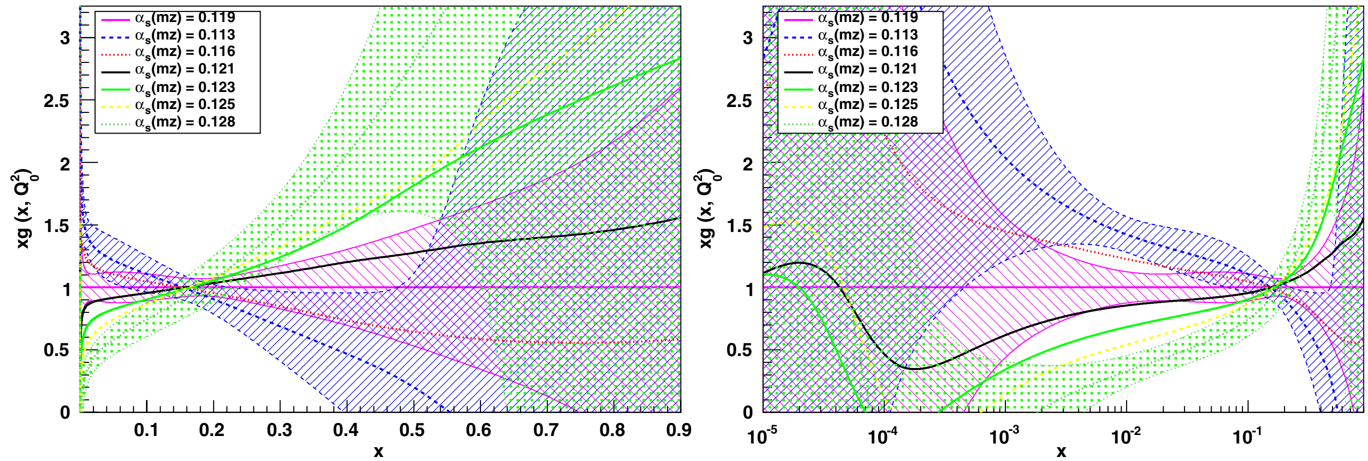


FIG. 2 (color online). The ratio of the central gluons obtained in NNPDF1.2 fits when $\alpha_s$ is varied, divided by the reference NNPDF1.2 gluon at the initial evolution scale $Q_0^2 = 2\ \mathrm{GeV}^2$. The comparison is shown both in a linear (left) and logarithmic (right) scales. One-$\sigma$ uncertainty bands are shown for the central, highest, and lowest values of $\alpha_s$.

the central CTEQ6.6 set. Therefore, it is possible to study the correlation between the value of $\alpha_s$ and PDFs, but not the correlation with their uncertainties.

The MSTW collaboration instead has performed a simultaneous determination of PDFs and $\alpha_s$, which is thus not treated as a fixed external parameter, but rather as a fit parameter, which leads to the central value quoted in Eq. (9). Furthermore, MSTW has also released sets of PDFs, analogous to the CTEQ sets discussed above, in which $\alpha_s$ is taken as an external parameter, and varied in steps of 0.001 for $0.110 \leq \alpha_s \leq 0.130$. The sets in which PDFs and $\alpha_s$ are determined simultaneously may be used for a determination of the correlation between the value of $\alpha_s$ and both PDF central values and PDF uncertainties, though with the limitation that the value and uncertainty on $\alpha_s$ found in the fit must be used.

### B. PDFs and $\alpha_s$ in a Monte Carlo approach

In the NNPDF parton determination, $\alpha_s$ is taken as a fixed parameter as in the CTEQ fits; the correlation between NNPDF1.2 PDFs and the value of $\alpha_s$ has been discussed recently in Ref. [18]. For the present work, we have constructed a family of NNPDF1.2 PDF sets using different values of $\alpha_s$. The very recent NNPDF2.0 PDF set [19] also includes PDFs determined with different fixed valued of $\alpha_s$.[2]

We have repeated the NNPDF1.2 PDF determination with $\alpha_s$ varied in the range $0.113 \leq \alpha_s \leq 0.128$ and all other aspects of the parton determination unchanged: for each value of $\alpha_s$ we have produced a set of 100 PDF replicas. In Fig. 2 we show the ratios of the central gluons obtained in these fits compared to the reference NNPDF1.2 gluon with $\alpha_s(M_Z) = 0.119$, together with the PDF uncertainty band which corresponds to the reference value.

The qualitative behavior of the gluon in Fig. 2 can be understood as follows. In NNPDF1.2, the gluon is determined by scaling violations of deep-inelastic structure functions, i.e. mostly from medium and small $x$ HERA data, with the large $x$ gluon constrained by the momentum sum rule. With a given amount of scale dependence seen in the data, smaller values of $\alpha_s$ require a larger small $x$ gluon, and thus because of the sum rule a smaller large $x$ gluon. In global fits [8,12,19] the behavior is essentially the same, up to the fact that some extra constraint on the large $x$ gluon is provided by Tevatron jet data, as quantified in [19].

The size of this correlation of the gluon with the value of $\alpha_s$ shown in Fig. 2 is clearly statistically significant; however, when $\alpha_s$ is varied within its uncertainty range, Eq. (10), the change in gluon distribution is generally smaller than the uncertainty on the gluon itself. It is interesting to note that the size of the uncertainty for values of $\alpha_s$ which are away from the best fit is often larger than the uncertainty when $\alpha_s$ is at or close to its best fit value: this is to be contrasted to what happens in a Hessian approach, where linear error propagation inevitably implies that the PDF uncertainty shrinks when $\alpha_s$ moves away from its best-fit value [12].

Given sets of replicas determined with different values of $\alpha_s$, it is possible to perform statistics in which $\alpha_s$ is varied, by assuming a distribution of values for $\alpha_s$. For instance, the average over Monte Carlo replicas of a general quantity which depends on both $\alpha_s$ and the PDFs, $\mathcal{F}(\mathrm{PDF}, \alpha_s)$ can be computed as

$$\langle \mathcal{F} \rangle_{\mathrm{rep}} = \frac{1}{N_{\mathrm{rep}}} \sum_{j=1}^{N_\alpha} \sum_{k_j=1}^{N_{\mathrm{rep}}^{\alpha_s^{(j)}}} \mathcal{F}(\mathrm{PDF}^{(k_j,j)}, \alpha_s^{(j)}), \qquad (12)$$

[2]The NNPDF1.2 sets with variable $\alpha_s$ are available upon request. The NNPDF2.0 sets with variable $\alpha_s$ are available from the webpage of the NNPDF Collaboration, htpp://sophia.ecm.ub.es/nnpdf, and is also available through the LHAPDF interface.

where $\mathrm{PDF}^{(k_j,j)}$ stands for the $k_j$th replica of the PDF fit with $\alpha_s = \alpha_s^{(j)}$, and the numbers $N_{\mathrm{rep}}^{\alpha_s^{(j)}}$ of replicas for each value of $\alpha_s$ in the total sample are determined by the probability distribution of values of $\alpha_s$, with the constraint

$$N_{\mathrm{rep}} = \sum_{j=1}^{N_{\alpha_s}} N_{\mathrm{rep}}^{\alpha_s^{(j)}}. \qquad (13)$$

Specifically, assuming that global fit values of $\alpha_s$ [such as

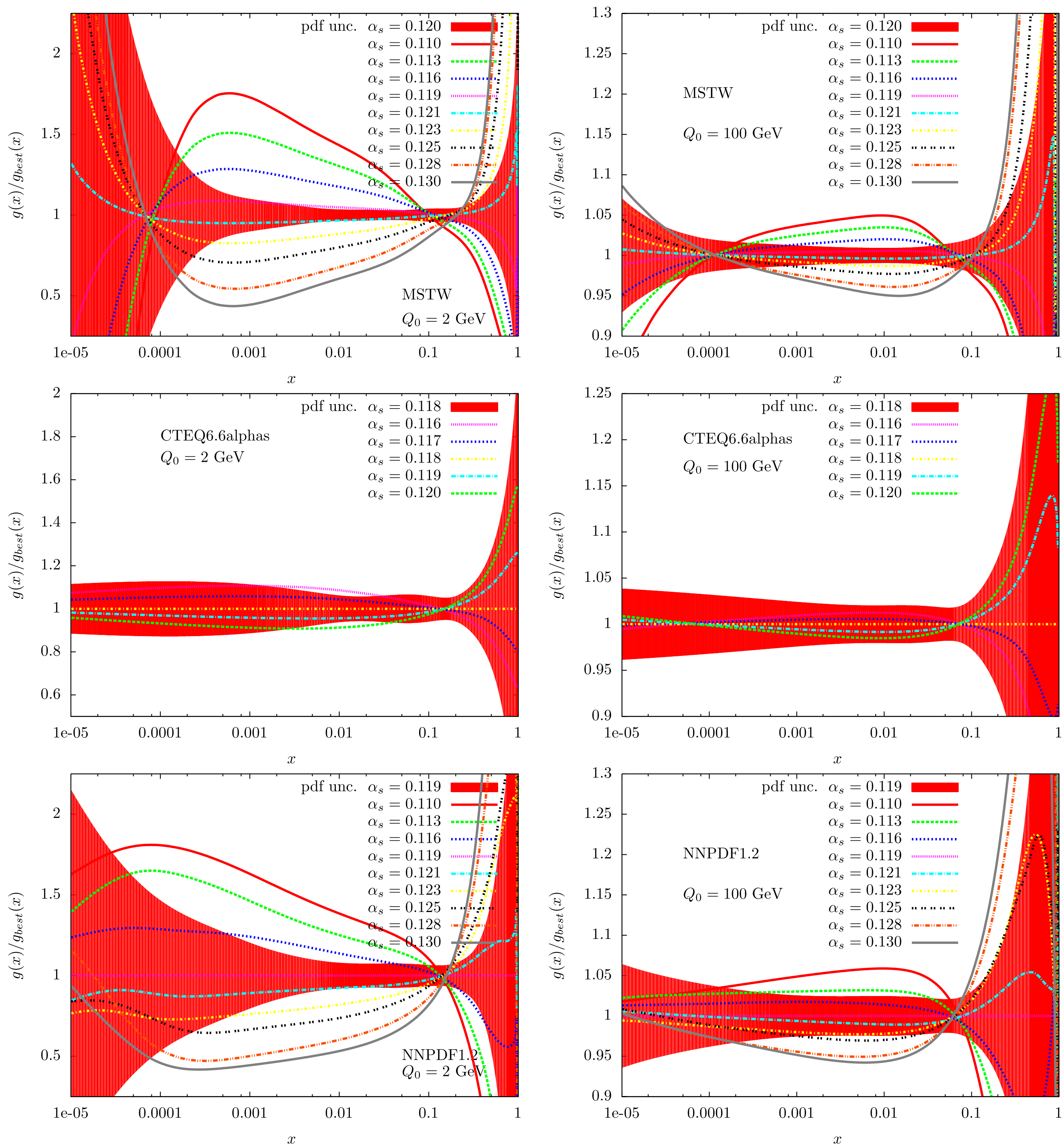


FIG. 3 (color online). Comparison of the gluon PDFs from MSTW08 (top), CTEQ6.6 (center), and NNPDF1.2 (bottom) at the scales $Q^2 = 4\ \mathrm{GeV}^2$ and $Q^2 = 10^4\ \mathrm{GeV}^2$ as $\alpha_s$ is varied, normalized to the corresponding central sets, determined with the value of $\alpha_s$ listed in Eq. (9). The one-$\sigma$ uncertainty band for the central set is also shown in each case.

Eqs. (7) and (8)] are Gaussianly distributed, the number of replicas is

$$N_{\rm rep}^{\alpha_s^{(j)}} \propto \exp\left(-\frac{(\alpha_s^{(j)} - \alpha_s^{(0)})^2}{2(\delta_{\alpha_s}^{(68)})^2}\right). \qquad (14)$$

with the normalization condition Eq. (13).

### C. Comparison of global PDF sets with variable $\alpha_s$

The dependence of the gluon distribution on the value of $\alpha_s$ is summarized in Fig. 3, where results obtained using the CTEQ6.6, MSTW08, and NNPDF1.2 $\alpha_s$ series are compared, both at the scale $Q^2 = 4\ \mathrm{GeV}^2$, close to the scale at which PDFs are parametrized, and at the high scale $Q^2 = 10^4\ \mathrm{GeV}^2$, typical of electroweak final states. The three central sets of Fig. 3 are then compared directly in Fig. 4. The gluon luminosities computed from these three central sets are then finally compared in Fig. 5 at Tevatron and LHC energies. The luminosities are plotted as a function of $m_H$ for given energy using the leading-order kinematic relation $x = m_H^2/s$. It should be borne in mind that, because of soft-gluon dominance [20], the NLO contribution is strongly peaked at the endpoint, and thus probes mostly the luminosity at the same value of $x$ as the LO.

Notable features of these comparisons are the following:

(i) The same correlation pattern between the gluon and $\alpha_s$ discussed for NNPDF in Sec. III B is also apparent for other sets.

(ii) At $Q^2 = 4\ \mathrm{GeV}^2$ uncertainties at very small $x$ for MSTW and NNPDF are large enough to swamp the $\alpha_s$ dependence. This does not happen for CTEQ, likely due to the more restrictive gluon parametrization used. However, at $Q^2 = 10^4\ \mathrm{GeV}^2$ the region at which uncertainties blow up is pushed to much smaller values of $x$.

(iii) Uncertainties at large $x$ also swamp the $\alpha_s$ dependence, due to the scarcity or (for NNPDF1.2) lack of data in this region.

(iv) Even in the medium $x$ region where the gluon is best known PDF uncertainty bands are rather larger than

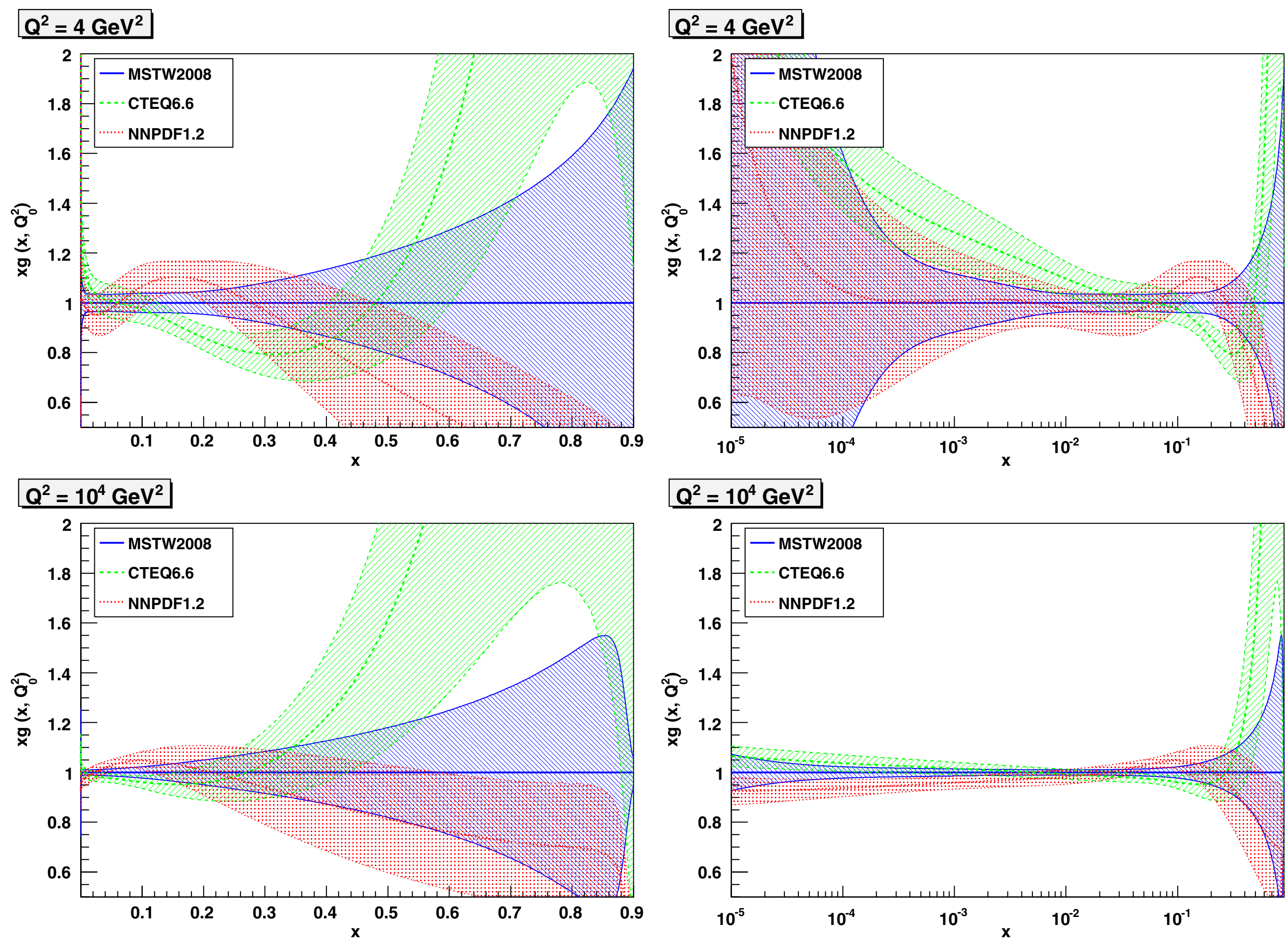


FIG. 4 (color online). Comparison of the gluon PDFs from MSTW08, CTEQ6.6, and NNPDF1.2 at the scales $Q^2 = 4\ \mathrm{GeV}^2$ (upper plots) and $Q^2 = 10^4\ \mathrm{GeV}^2$ (lower plots), each determined with the value of $\alpha_s$ listed in Eq. (9), all normalized to the central MSTW08 set.

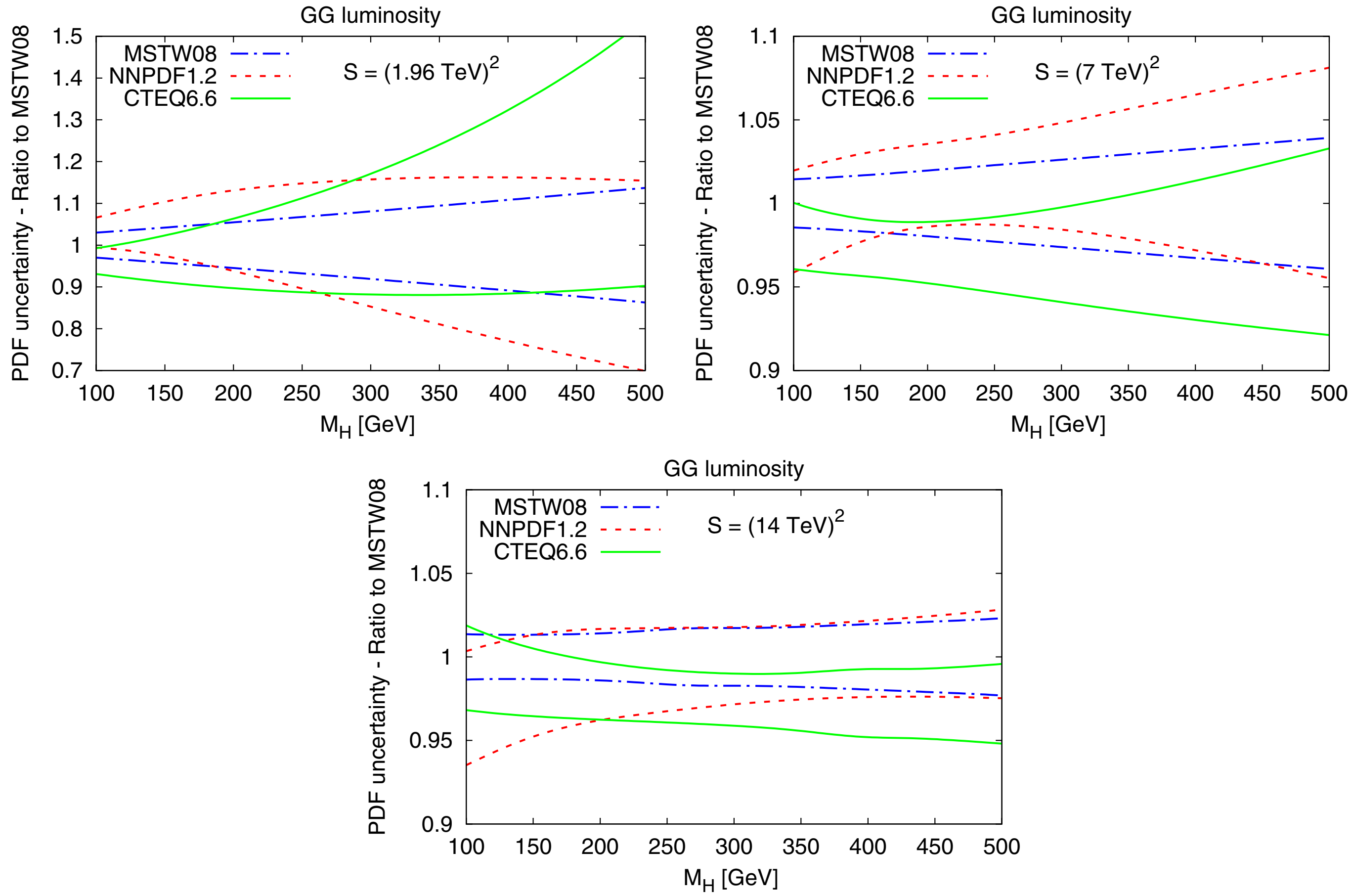


FIG. 5 (color online). Comparison of the gluon luminosities from MSTW08, CTEQ6.6, and NNPDF1.2 at the Tevatron (upper left plot), LHC 7 TeV (upper right plot) and LHC 14 TeV (lower plot) and $Q^2 = 10^4$ GeV$^2$, each determined with the value of $\alpha_s$ listed in Eq. (9), all normalized to the central MSTW08 set.

the gluon variation due to the variation of $\alpha_s$ within its uncertainty Eq. (7) or even Eq. (8).

(v) The three gluons in Fig. 4 overlap to one-$\sigma$ in most of the kinematic region. However, at low scale they disagree significantly at large $x$, and at high scale they disagree, though by less than about two $\sigma$, both at very large and very small $x$.

(vi) Once gluons are convoluted into a parton luminosity, most of the disagreements seen in Fig. 4 are washed out: indeed, the parton luminosities Fig. 5 computed from CTEQ6.6, MSTW08, and NNPDF1.2 all agree within uncertainties, in the sense that their one-$\sigma$ error bands always overlap (though sometimes just about).

### D. Correlation between PDFs and $\alpha_s$

Correlations between different PDFs, or between PDFs and physical observables, have been computed by CTEQ using a Hessian approach [8], and by NNPDF using a Monte Carlo approach [10]. Within a Monte Carlo approach it is in fact easy to estimate the correlation between any pair of quantities by computing their covariance over the Monte Carlo sample. Statistics involving the value of $\alpha_s$ can then be performed provided only replicas with different values of $\alpha_s$ are available, as discussed in Sec. III B above, Eq. (12).

Indeed, in a Monte Carlo approach the correlation between the strong coupling and the gluon (or any other PDF) is given by

$$\rho[\alpha_s(M_Z^2), g(x, Q^2)] = \frac{\langle \alpha_s(M_Z^2) g(x, Q^2)\rangle_{\rm rep} - \langle \alpha_s(M_Z^2)\rangle_{\rm rep}\langle g(x, Q^2)\rangle_{\rm rep}}{\sigma_{\alpha_s(M_Z^2)}\sigma_{g(x,Q^2)}}, \tag{15}$$

where the distribution of values of $\alpha_s$ is automatically reproduced if one picks $N_{\rm rep}^{\alpha_s^{(j)}}$ of replicas for each value of $\alpha_s$ according to Eqs. (13) and (14) above.

Our results for the correlation coefficient between the gluon and $\alpha_s(M_Z)$ as a function of $x$, computed using Eq. (15), with the NNPDF1.2 PDFs of Sec. III B and

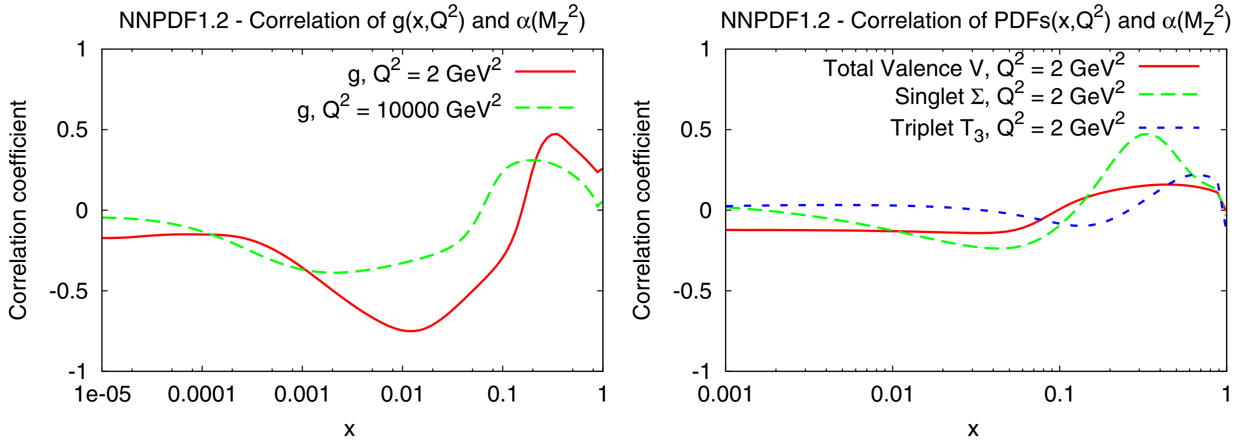


FIG. 6 (color online). The correlation Eq. (15) between PDFs and $\alpha_s(M_Z)$ as a function of $x$. Left: gluon PDF at $Q^2 = 2$ GeV$^2$ and $Q^2 = 10^4$ GeV$^2$; right: singlet, triplet, and total valence PDFs for $Q^2 = 2$ GeV$^2$.

Eq. (10) for $\alpha_s$, both at a low scale $Q^2 = 2$ GeV$^2$ and at a typical LHC scale $Q^2 = 10^4$ GeV$^2$, are shown in Fig. 6. It is interesting to note how evolution decorrelates the gluon from the strong coupling. We also show in Fig. 6 the correlation coefficient for other PDFs: as expected for the triplet and valence PDFs it is essentially zero, that is, in NNPDF1.2 these PDFs show essentially no sensitivity to $\alpha_s$. The correlation coefficient Fig. 6 quantifies the qualitative observations of Fig. 2.

## IV. THE CROSS SECTION: PDF UNCERTAINTIES

We now turn to the computation of the Higgs production cross section and associate uncertainty band due to PDF variation, with $\alpha_s$ kept fixed at each group's preferred value, as given by Eq. (9), and uncertainties consistently determined as one-$\sigma$ intervals using each groups recommended method, hence, in particular, Hessian methods for CTEQ and MSTW and Monte Carlo methods for NNPDF. We will not address here the issue of comparison of the various methods, and we will simply take each group's results at face value, in particular, by taking as a 68% confidence level the interval determined as such by each group. When comparing results it should be borne in mind that, as discussed in Sec. III C, the cross sections probe the gluon luminosity at an essentially fixed value of $x = m_H^2/s$.

### A. Comparison of cross sections and uncertainties

In Fig. 7 we compare the cross sections at Tevatron and LHC (7 TeV and 14 TeV) energies as a function of the Higgs mass; each cross section is calculated using the best PDF set of each group and the corresponding value of $\alpha_s$ of Eq. (9) in the determination of the hard cross section. Central values can differ by a sizable amount. Discrepancies are due to three distinct reasons: the fact that the hard cross sections (independent of the PDF) are different because of the different values of $\alpha_s$; the fact that the PDFs are different because they depend on $\alpha_s$ as shown in Figs. 3; lastly, the fact that, even when the same value of $\alpha_s$ is adopted, PDF determination from different groups do not coincide.

As discussed in Sec. III, the first two effects tend to compensate each other at small $x$ because of the anticorrelation between the gluon and $\alpha_s$ (see Fig. 6), while at large $x$ they go in the same direction. As we shall see in Sec. V B, the transition between anticorrelation to correlation happens for LHC 7 TeV for intermediate values of the Higgs mass.

The relative impact of the first effect (which affects the hard cross section) and of the second two combined (which affect the parton luminosity) can be assessed by comparing the cross sections of Fig. 7 with the luminosities of Fig. 5: for instance, for $m_H = 150$ GeV at the LHC (7 TeV), the MSTW08 cross section is seen in Fig. 7 to be by about 7% higher than the CTEQ6.6 one. Of this, Fig. 5 shows that about 3% is due to the different parton luminosity, hence about 4% must be due to the choice of $\alpha_s$ in the hard matrix element. In Sec. V B we will determine this variation directly (Fig. 10) and see that this is indeed the case.

Because the cross section starts at order $\alpha_s^2(m_H)$, with a NLO $K$-factor of order one, we expect a percentage change $\Delta\alpha_s$ in $\alpha_s$ to change the cross section by about $2.5\Delta\alpha_s$, which indeed suggests a 4% change of the hard cross section when $\alpha_s$ is changed from the MSTW08 to the CTEQ6.6 value. In fact, comparison of Fig. 7 to Fig. 5 shows that this simple estimate works generally quite well: the difference in hard matrix elements is $2.5\Delta\alpha_s$, so 4% when moving from the MSTW08 to the CTEQ6.6 value, with the rest of the differences seen in the cross sections in Fig. 7 due to the gluon luminosities displayed in Fig. 5. Because the latter are compatible to one-$\sigma$, this is already sufficient to show that nominal uncertainties on PDF sets are sufficient to accommodate the different central values of NNPDF1.2, CTEQ6.6, and MSTW08 once a common value of $\alpha_s$ is adopted.

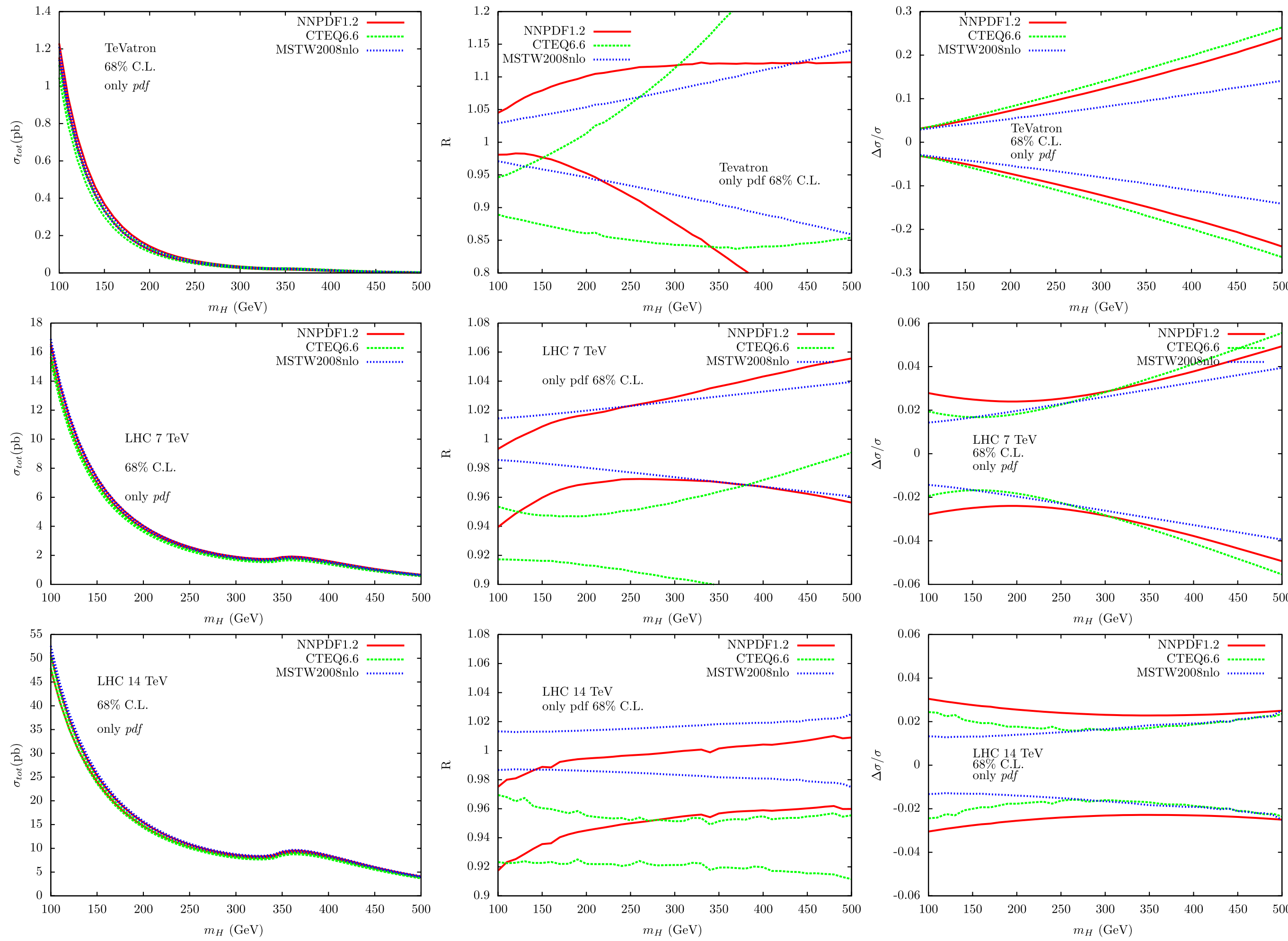


FIG. 7 (color online). Cross sections for Higgs production from gluon-fusion at the Tevatron (top), LHC 7 TeV (center), and LHC 14 TeV (bottom). All uncertainty bands are one-$\sigma$ PDF uncertainties, with $\alpha_s$ fixed according to Eq. (9). The left column shows absolute results, the central column results normalized to the MSTW08 result, and the right column results normalized to each group's central result.

Uncertainties turn out to be quite similar for all groups and of order of a few percent, with uncertainties largest at the Tevatron for large Higgs mass. The growth of uncertainties as the Higgs mass is raised or the energy is lowered is due to the fact that larger $x$ values are then probed, where knowledge of the gluon is less accurate, as shown in Fig. 4.

### B. The uncertainty of the PDF uncertainty bands

In order to answer the question of the compatibility of different determinations of PDFs or of physical observables extracted from them it is important that the uncertainties are provided on the quantities which are being compared. Whereas this is standard for central values, it is less frequently done for uncertainties themselves. A systematic way of doing so in a Monte Carlo approach has been introduced in Refs. [10,19] (see, in particular, Appendix A of [19]): the difference between two determinations of a central value or an uncertainty is compared to the sum in quadrature of the uncertainty on each of the two quantities. Only when this ratio is significantly larger than 1 is the difference significant.

It is important to observe that, when addressing the compatibility of two determinations, two inequivalent questions can be asked: whether the two determinations come from statistically indistinguishable underlying distributions, or whether they come from statistically distinguishable distributions, but are nevertheless compatible. To elucidate the difference, consider two different determinations of the same quantities based on two independent sets of data. If the data sets are compatible, the two determinations will be consistent within uncertainties in the sense that the central values are compatible within uncertainties (i.e. the central values will be distributed compatibly to the given uncertainty if many determinations are compared). However, the underlying distribution of results will in general be different: for example, if one of the two data sets is more accurate than the other, the two distributions will certainly be statistically inequivalent (they will have different width), yet they may well be compatible. We expect complete statistical equivalence of two different PDF determinations only if they are based on the same data and methodology: for example, NNPDF verifies that its PDF determination is statistically independent of the architecture of the neural networks which are used in the analysis. However, when comparing determinations which use different data sets, PDF parametrization, minimization algorithm etc., we only expect them to be compatible, but not statistically indistinguishable.

The uncertainty on the uncertainty is introduced in order to be able to answer either of these two questions in a quantitative way [10,19]: it provides the unit in which one can measure the distance between two different determinations of PDF uncertainties, and thus assess whether (a) they come from the same underlying distribution or (b) whether they come from different, but compatible underlying distribution. We will refer to the former as ''uncertainty on the mean uncertainty'' (statistical equivalence) and to the latter as ''uncertainty on the PDF uncertainty'' (compatibility).

The determination of the uncertainty on the uncertainty appears to be nontrivial in a Hessian approach, and it has not been addressed so far in the context of Hessian PDF determination to the best of our knowledge. We will thus only discuss it within a Monte Carlo framework and present results for NNPDF. However, it seems plausible then to assume that uncertainties on uncertainties are of similar size in existing parton fits, so that the results for other parton fits should not be too different.

The determination of the uncertainty on the uncertainty in a Monte Carlo approach has been discussed in detail in Appendix A of Ref. [19], to which we refer for a more detailed treatment. Here, we recall that, given a set of $N_{\rm rep}$ replicas, the uncertainty on the mean uncertainty (used to assess statistical equivalence) coincides with the variance of the variance, which in turn is given by [6]

$$\sigma^2[\sigma^2] = \frac{1}{N_{\rm rep}}\left[m_4[q] - \frac{N_{\rm rep}-3}{N_{\rm rep}-1}(\bar{\sigma}^2)^2\right], \tag{16}$$

where $\sigma^2$ and $m_4$ are, respectively, the variance and fourth moment of the replica sample. Equivalently, $\sigma^2[\sigma^2]$ can be determined using the jackknife method (see e.g. Ref. [21]), i.e. removing one of the replicas from the sample and determining the $N_{\rm rep}$ variances

$$\sigma_i^2(x) = \frac{1}{N_{\rm rep}-2}\sum_{j=1, j\neq i}^{N_{\rm rep}}(x_j - \mu_i(x))^2; \quad i = 1, \ldots, N_{\rm rep}. \tag{17}$$

The variance of the variance is then given by

$$\sigma^2[\sigma^2] = \sum_{i=1}^{N_{\rm rep}}[(\sigma_i^2)^2 - \bar{\sigma}_i^4], \tag{18}$$

where $\sigma_i^2$ is given by Eq. (17) and

$$\bar{\sigma}_i^4 = \frac{1}{N_{\rm rep}}\sigma_i^4. \tag{19}$$

The uncertainty on the PDF uncertainty is larger by a factor $\sqrt{N_{\rm rep}}$ than the uncertainty on the mean uncertainty [19]. To understand this, note that latter vanishes in the limit $N_{\rm rep} \to \infty$, while the former does not: indeed, if the two replica sets come from the same underlying distributions, all quantities computed from them should coincide in the infinite-sample size limit, while if they merely come from compatible distributions even for very large sample quantities computed from them should remain different. In summary, the quantity which should be used to assess statistical equivalence is $\sigma[\sigma^2]$, while the quantity which should be used to assess consistency is $\sqrt{N_{\rm rep}}\sigma[\sigma^2]$.

In Fig. 8 we plot the relative uncertainty on the cross section, supplemented by a band whose width coincides with the uncertainty on the mean uncertainty $\sigma[\sigma^2]$, as given by Eq. (18), all computed using the NNPDF1.2 sets with different values of $\alpha_s$. We can immediately conclude from this figure that the mean uncertainty on the cross sections does not change in a statistically significant way when $\alpha_s$ is varied within the range Eq. (7) or even Eq. (8): $\alpha_s$ has to be varied by about 3 times the range Eq. (8) for the mean uncertainty on the cross section to change in a statistically significant way. Incidentally, this plot also shows that uncertainties are not necessarily smaller (and

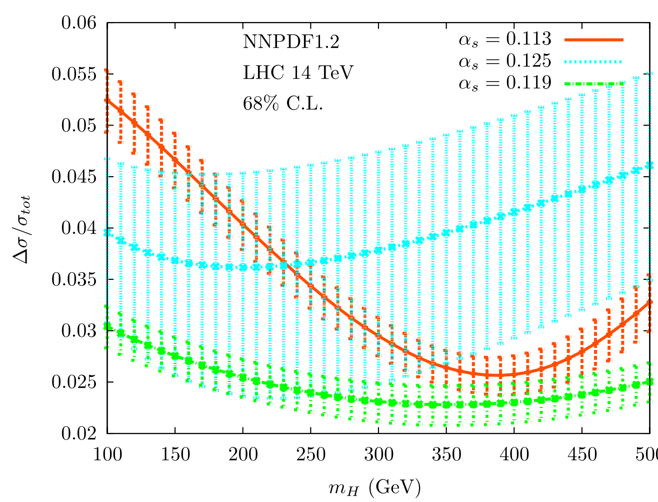


FIG. 8 (color online). The uncertainty on the Higgs cross section determined using NNPDF1.2 with different values of $\alpha_s$. The width of the band shown denotes the statistical uncertainty on the mean uncertainty of the sample, $\sigma[\sigma^2]$, Eq. (17). Note that the uncertainty on the PDF uncertainty is $\sqrt{N_{\rm rep}} = 10$ times larger.

in fact are mostly larger) when $\alpha_s$ is varied away from its preferred value, as already seen in Sec. III B and Fig. 2.

As discussed above, when assessing compatibility (as opposed to statistical equivalence) of PDF sets, the size of the uncertainty bands shown in Fig. 8 must be rescaled up by a factor $\sqrt{N_{\rm rep}} = 10$. These rescaled uncertainties on the PDF uncertainty are then more then half of the PDF uncertainty itself. This means that all PDF uncertainties shown in Fig. 7 for the three PDF fits under investigation are in fact compatible with each other at the one-$\sigma$ level, since they differ at most by a factor two (NNPDF vs MSTW at LHC 14 TeV and the lowest values of $m_H$), and in fact usually rather less than that.

## V. THE CROSS SECTION: $\alpha_s$ UNCERTAINTIES

We have seen in the previous section (see Fig. 7) that once differences in hard matrix elements due to the different choice of $\alpha_s$ are accounted for, cross sections computed using different parton sets agree to one-$\sigma$ because parton luminosities do. However, parton luminosities compared in Fig. 5 were determined using the different values of $\alpha_s$ Eq. (9).

For a fully consistent comparison, we must determine central parton luminosities (and thus cross sections) with a common value of $\alpha_s$, thereby isolating the differences which are genuinely due to PDFs. The uncertainty related to the choice of $\alpha_s$ must then be determined by variation around the central value. This then raises the question of the correlation between this $\alpha_s$ variation and the values of the PDFs and their uncertainties. We now address all these issues in turn.

### A. The cross section with a common $\alpha_s$ value

The cross sections obtained from the three PDF sets under investigation at the same value of $\alpha_s$ are compared in Fig. 9, where the ratios of cross sections computed using in the numerator and denominator two different PDF sets (NNPDF1.2 vs MSTW08 and CTEQ6.6 vs MSTW08) are shown for different choices of $\alpha_s$.

Comparison of these ratios to the PDF uncertainties shown in Fig. 7 show that they are typically of a similar size: namely, 2%–3% at the LHC, while at the Tevatron they are about twice as large for light Higgs mass, rapidly growing more or less linearly, up to about 10% around the top threshold. The largest discrepancy in comparison to the PDF uncertainties is found at the lowest Higgs masses at the Tevatron between the CTEQ and MSTW sets, whose uncertainty bands barely overlap there. This can be traced to the behavior of the gluon luminosities of Fig. 5.

Hence, the spread of central values obtained using the PDF sets under investigation is consistent with their uncertainties, which are thus unlikely to be incorrectly estimated. Of course, it should be borne in mind that these uncertainties are in turn estimated with a finite accuracy, unlikely to be much better than 50%, as seen in Sec. IV B.

### B. Uncertainty due to the choice of $\alpha_s$

The simplest way to estimate the uncertainty due to $\alpha_s$ is to take it as uncorrelated to the PDF uncertainty, and determine the variation of the cross section as $\alpha_s$ is varied. This, in turn, can be done either by simply keeping the PDFs fixed, or else by also taking into account their correlation to the value of $\alpha_s$ discussed in Sec. III, i.e. by using for each value of $\alpha_s$ the corresponding best-fit PDF set. In either case, the uncertainty on the cross section due to the variation of $\alpha_s$ is

$$(\Delta\sigma)^{\pm}_{\alpha_s} = \sigma(\alpha_s \pm \Delta\alpha_s) - \sigma(\alpha_s), \tag{20}$$

with, in the two cases, the cross section computed either with a fixed set of PDF, or with the sets of PDFs corresponding to the three values $\alpha_s \pm \Delta\alpha_s$.

We have determined $(\Delta\sigma)^{\pm}_{\alpha_s}$ Eq. (20) using the central value of $\alpha_s$ of Eq. (10) and $\Delta\alpha_s = 0.002$, which would correspond to a 90% C.L. variation of $\alpha_s$ according to Eq. (11), and it is (almost exactly) equal to the difference between the preferred values of $\alpha_s$ for CTEQ6.6 and MSTW08, Eq. (9). For NNPDF1.2 a PDF set with $\alpha_s = 0.117$ is not available, hence the lower cross section in the case in which the PDFs are varied has been determined by a suitable rescaling of that which corresponds to $\alpha_s = 0.116$.

Results for LHC 7 TeV are shown in Fig. 10: upper and lower cross sections correspond to the upper and lower values of $\alpha_s$, but the variation turns out to be symmetric about the central value to good approximation. If the PDF is kept fixed, we find $(\Delta\sigma)^{\pm}_{\alpha_s}/\sigma \approx 0.04$ when $\Delta\alpha_s = 0.002$, *i.e.* a variation of about 4%, in excellent agreement with the simple estimate of Sec. IV A. If the PDFs are also varied, the width of the uncertainty band on the cross section for light Higgs becomes smaller, because of the anticorrelation of the small $x$ gluon to $\alpha_s$ discussed in Sec. III (see Fig. 6), but it becomes wider as the Higgs mass is raised and larger $x$ values are probed, for which the correlation of gluon to $\alpha_s$ is positive.

### C. Impact of $\alpha_s$ on uncertainties

So far we have considered the uncertainties due to PDFs and due to the value of $\alpha_s$ separately. However, as seen in Sec. III, when $\alpha_s$ changes, not only the central values but also the uncertainties on PDF change, and this leads to a correlation between PDF and $\alpha_s$ uncertainties. The effect of this correlation on the determination of combined PDF + $\alpha_s$ uncertainties is likely to be moderate: it is a higher order effect, and the dependence of uncertainties on $\alpha_s$ is weak, especially if compared to the their own uncertainty, see Fig. 8.

We will now quantify this correlation by computing the total PDF + $\alpha_s$ uncertainty when the correlation is kept into account, and comparing results to those obtained when PDF and $\alpha_s$ uncertainties are added in quadrature. As

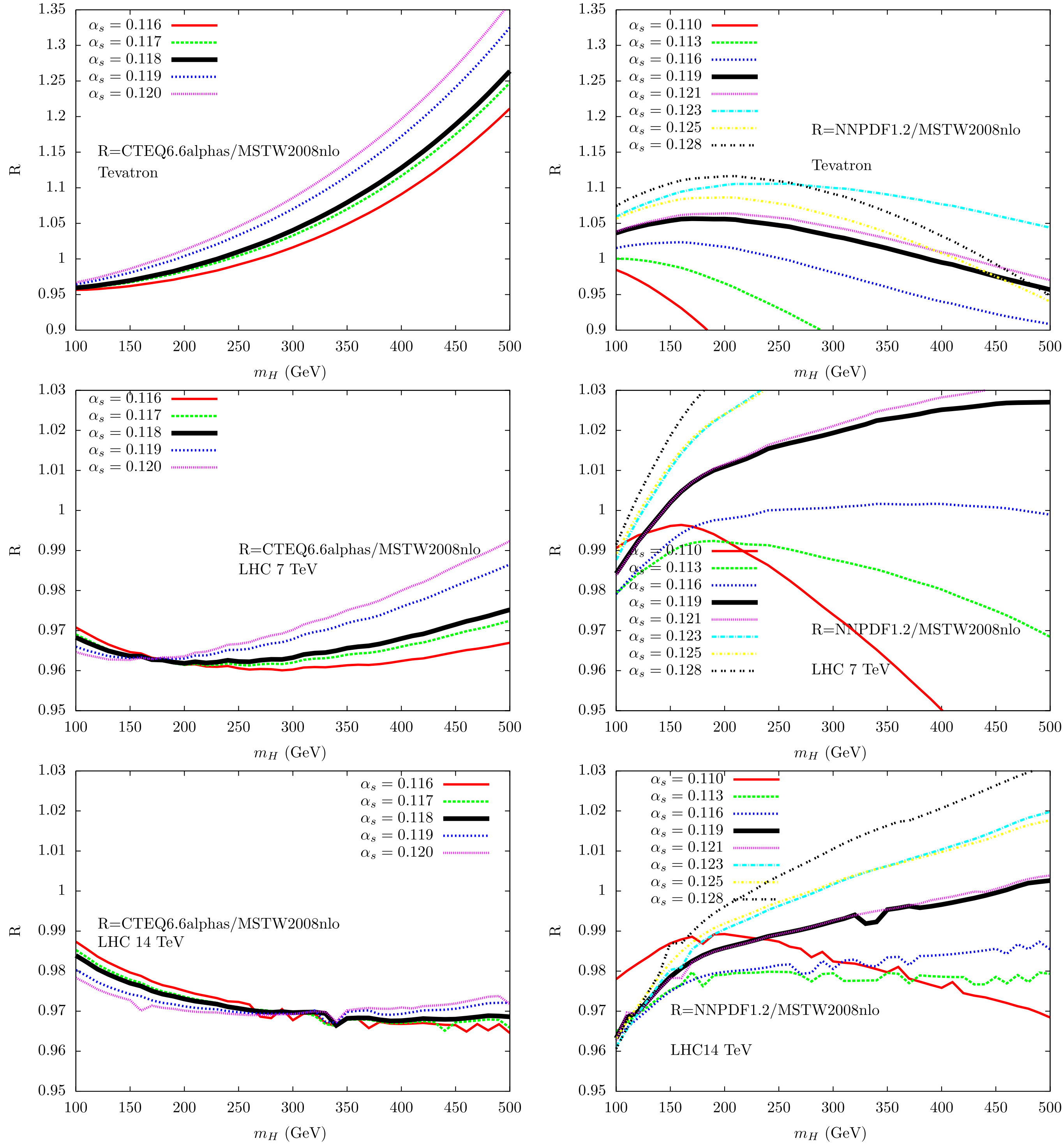


FIG. 9 (color online). Ratio of the Higgs production cross sections determined using PDFs from different groups, but obtained with the same value of $\alpha_s$: CTEQ6.6/MSTW08 (left) and NNPDF1.2/MSTW08 (right). Results are shown for different values of $\alpha_s$, and for the Tevatron (top), LHC 7 TeV (center), and LHC 14 TeV (bottom).

discussed in Sec. III, the correlated uncertainty can be determined both in the Hessian approach using MSTW08 and in a Monte Carlo approach using NNPDF. In the MSTW methodology this is done by relying on a simultaneous determination of PDFs and $\alpha_s$. As a consequence, the value and range of variation of $\alpha_s$ must be those obtained in this determination. This will not hamper our analysis in that the MSTW08 value and range for $\alpha_s$ of Ref. [12] are close to those under consideration. With the NNPDF methodology we are free to choose any value and

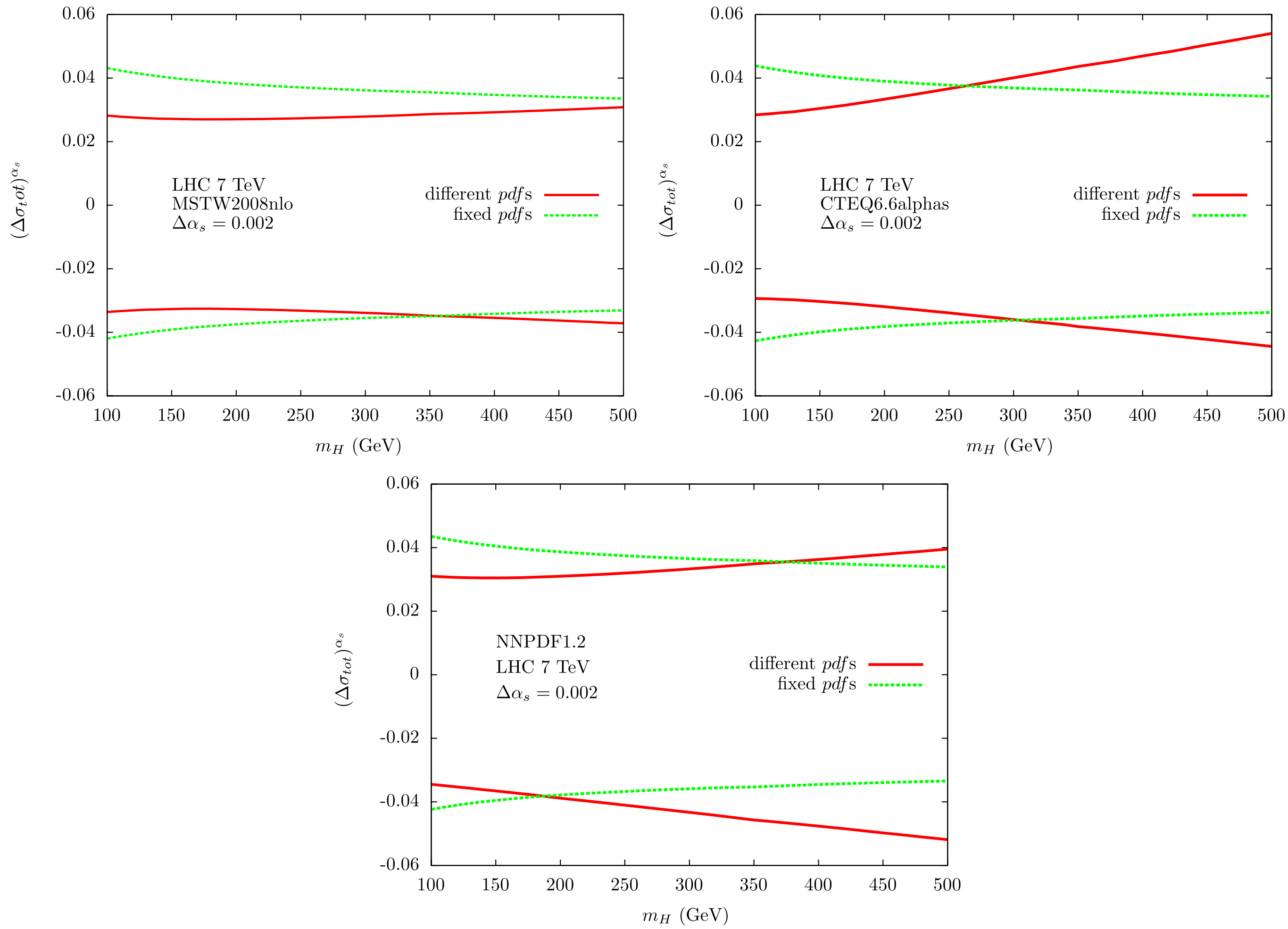


FIG. 10 (color online). Relative variation $\Delta\sigma/\sigma$ Eq. (20) of the cross section due to a variation $\Delta\alpha_s = 0.002$ about the preferred value Eq. (10) adopted by each PDF set. Results are shown both with PDFs kept fixed (dashed bands), or with the best-fit PDF set corresponding to each value of $\alpha_s$ (solid bands).

range for $\alpha_s$, inasmuch as the corresponding Monte Carlo PDF replicas are available.

We have thus computed joint PDFs + $\alpha_s$ uncertainties on the Higgs cross section. For MSTW08 we have followed the procedure of Ref. [12]: the total upper and lower (generally asymmetric) uncertainties on an observable $F$ are determined as

$$(\Delta F)_+^{\mathrm{PDF}+\alpha_s} = \max_{\alpha_s}(\{F^{\alpha_s}(S_0) + (\Delta F_{\mathrm{PDF}}^{\alpha_s})_+\}) - F^{\alpha_s^0}(S_0)$$
$$(\Delta F)_-^{\mathrm{PDF}+\alpha_s} = F^{\alpha_s^0}(S_0) - \min_{\alpha_s}(\{F^{\alpha_s}(S_0) - (\Delta F_{\mathrm{PDF}}^{\alpha_s})_-\},) \quad (21)$$

where $F^{\alpha_s}(S_0)$ is the observable computed using the central PDF set $S_0$ and the value $\alpha_s$ of the strong coupling, $(\Delta F_{\mathrm{PDF}}^{\alpha_s})_\pm$ is the PDF uncertainty on the observable for given fixed value of $\alpha_s$, as determined from the Hessian PDF eigenvectors [9,12], and the maximum and minimum are determined from a set of five results, each computed with one distinct value of $\alpha_s$ (central,$\pm$ half confidence level, $\pm$ confidence level). The value of $\alpha_s^0$ is as given in Eq. (9), while its one-$\sigma$ upper and lower variations are

$$\Delta^{(68)}\alpha_s = \begin{matrix} +0.0012 \\ -0.0015 \end{matrix}. \quad (22)$$

For NNPDF, the uncertainty is simply given by the standard deviation of the joint distribution of PDF replicas and $\alpha_s$ values

$$\Delta F^{\mathrm{PDF}+\alpha_s} = \sigma_F$$
$$\equiv \left[\frac{1}{N_{\mathrm{rep}}-1}\sum_{j=1}^{N_\alpha}\sum_{k_j=1}^{N_{\mathrm{rep}}^{\alpha_s^{(j)}}}(F[\{q^{(k_j,j)}\}] - F[\{q^0\}])^2\right]^{1/2} \quad (23)$$

where the number of replicas $N_{\mathrm{rep}}^{\alpha_s^{(j)}}$ for each value $\alpha_s^{(j)}$ of the strong coupling is determined in the Gaussian case by Eq. (14). In this case, we have taken as central value and

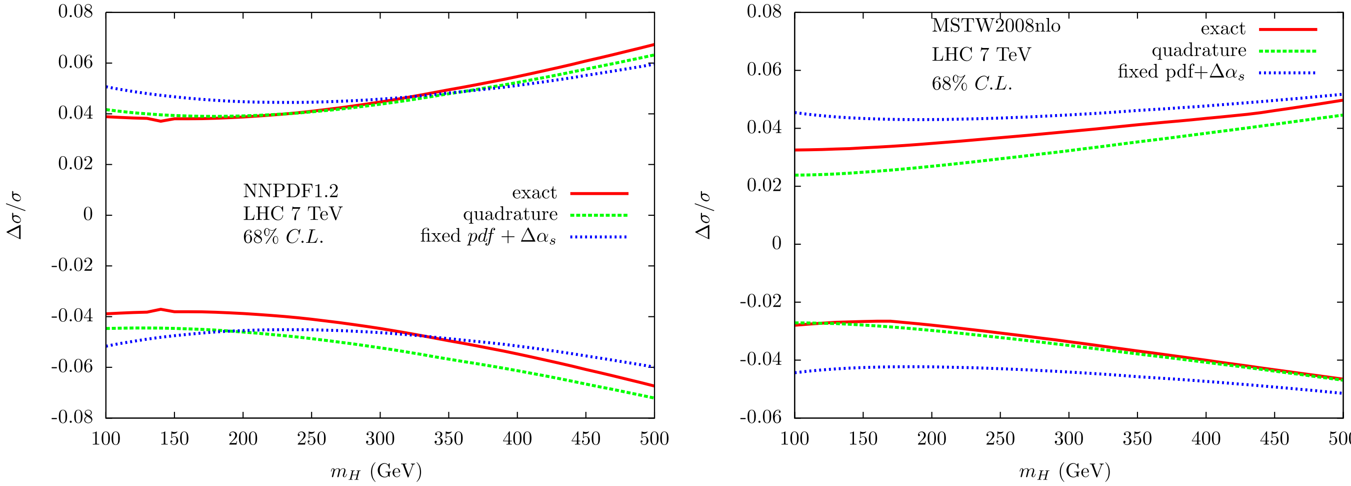


FIG. 11 (color online). The combined PDF + $\alpha_s$ relative one-$\sigma$ uncertainty on the Higgs cross section with NNPDF1.2 (left) and MSTW08 (right). The three bands correspond to results obtained keeping into account the full correlation between $\alpha_s$ and PDF uncertainties (exact), by adding in quadrature PDF uncertainties and $\alpha_s$ uncertainties in turn determined by keeping into account the correlation between $\alpha_s$ and PDF central values (quadrature), and finally by adding in quadrature PDF uncertainties and $\alpha_s$ uncertainties determined with PDFs fixed at their central value (fixed PDF + $\Delta\alpha_s$). The central values of $\alpha_s$ are given by Eq. (9), and its one-$\sigma$ range is in Eq. (10) in all cases except the MSTW08 exact for which it is given in Eq. (22).

uncertainty on $\alpha_s$ those given in Eqs. (9) and (10) respectively.

The results for the uncertainty obtained in this way are shown in Fig. 11, each normalized to the corresponding central cross section. They are compared to results obtained adding in quadrature the PDF uncertainties displayed in Fig. 7 and the $\alpha_s$ uncertainties Eq. (20) displayed in Fig. 10, in turn obtained either with fixed PDFs, or by taking the PDF set that corresponds to each value of $\alpha_s$. Note that the range of $\alpha_s$ variation for the MSTW08 curve with full correlation kept into account, given in Eq. (22), differs slightly from that, Eq. (10), used in all other cases. The effect of the correlation between $\alpha_s$ and PDF uncertainties is indeed quite small: as one might expect, it is in fact smaller than the effect of the correlation between $\alpha_s$ and PDF central values shown in Fig. 10, and much smaller than the uncertainty on the PDF uncertainty discussed in Sec. IV B.

## VI. THE CROSS SECTION: FINAL RESULTS

Our final results for the Higgs cross section are collected in Fig. 12: the cross sections are the same of Fig. 7, but now with the total PDF + $\alpha_s$ uncertainty. This is computed taking fully into account the correlation between $\alpha_s$, PDF central values and uncertainties for NNPDF and MSTW (as discussed in Sec. V C and shown in Fig. 10). For CTEQ, which does not provide error sets for each value of $\alpha_s$, the PDF uncertainties (Fig. 7) and $\alpha_s$ uncertainties (Sec. V B and Fig. 10) are added in quadrature; however, as seen in Sec. V C, this makes little difference.

The main features of these final results are the following:

(i) The total uncertainty on the cross section found by various groups are in reasonable agreement, especially if one recalls that they are typically affected by an uncertainty of order of about half their size, as seen in Sec. IV B. This follows from the fact that the total uncertainty is close to the sum in quadrature of the PDF and $\alpha_s$ uncertainties, with the $\alpha_s$ uncertainty essentially the same for all PDF sets, and PDF uncertainties on the input parton luminosity quite close to each other.

(ii) The predictions obtained using the three given sets all agree within the total PDF + $\alpha_s$ one-$\sigma$ uncertainty. This is a consequence of the fact that the central values of the cross section computed using the same value of $\alpha_s$ for all sets agree within PDF uncertainties, and that the spread of central values of $\alpha_s$ used by the three groups Eq. (9) is essentially the same as the $\alpha_s$ uncertainty under consideration.

The results shown in Fig. 12 can be combined into a determination of the cross section and its combined PDF + $\alpha_s$ uncertainty. We have seen that there is reasonably good agreement between the parton sets under investigation: apparent disagreement is only found if one compares results obtained with values of $\alpha_s$ which differ more than the uncertainty on $\alpha_s$. However, in some cases (for example at the Tevatron for light Higgs) the agreement is marginal: the one-$\sigma$ uncertainty bands just about overlap. Ideally, this situation should be resolved by the PDF fitting groups by investigating the origin of the underlying imperfect agreement of parton luminosity. However, until this is done, a common determination of the cross section with a more conservative estimate of the uncertainty may be obtained by suitably inflating the PDF uncertainty.

We have considered two different procedures which lead to such a common determination, based on the idea of

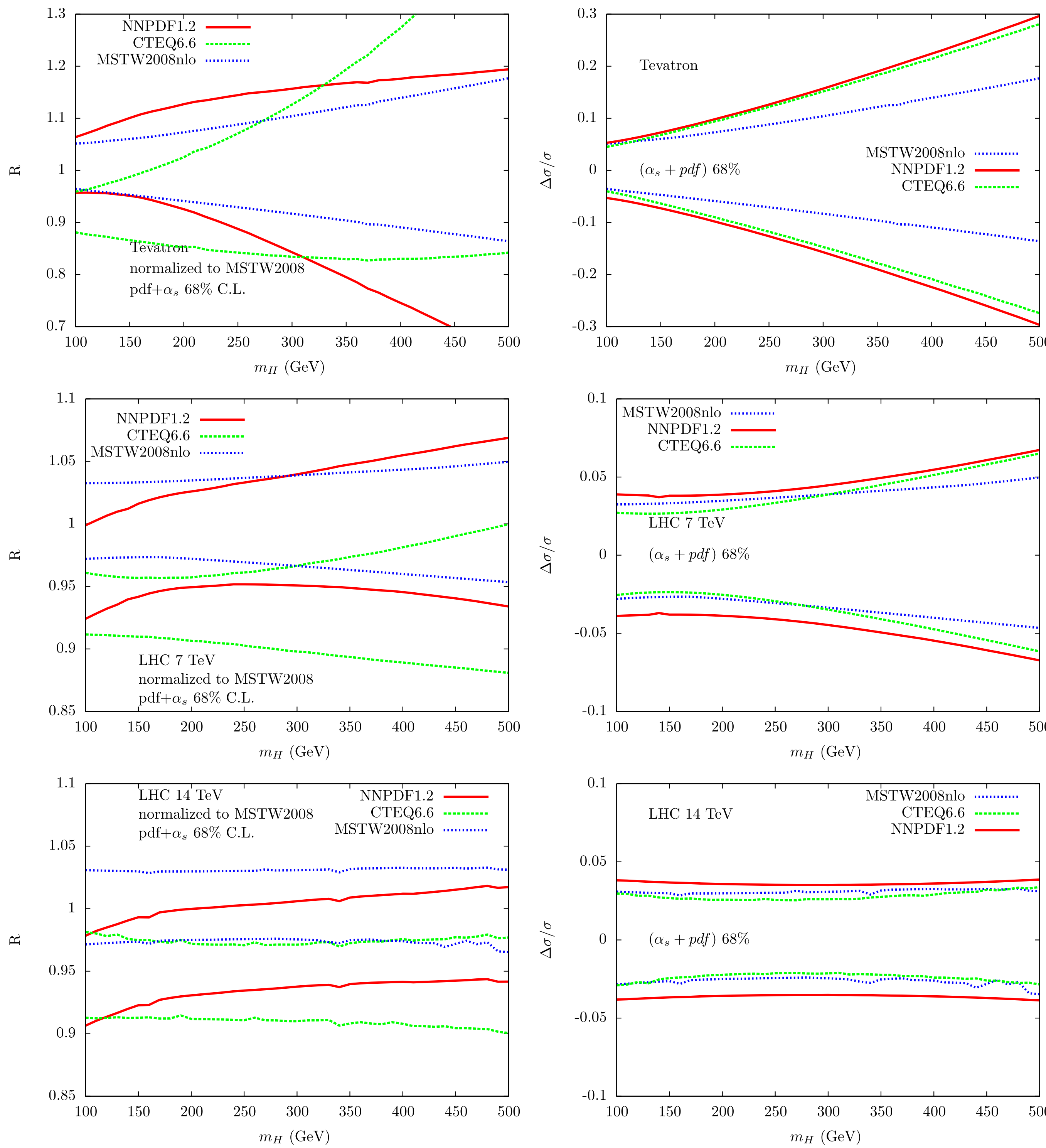


FIG. 12 (color online). Cross sections for Higgs production from gluon-fusion at the Tevatron (top), LHC 7 TeV (center), and LHC 14 TeV (bottom). All uncertainty bands are one-$\sigma$ combined PDF + $\alpha_s$ uncertainties, as in Fig. 11 (exact) for MSTW and NNPDF, and as in Fig. 10 for CTEQ, with the central value of $\alpha_s$ of Eq. (9). The left column shows results normalized to the MSTW08 result, and the right column results normalized to each group's central result (relative uncertainty).

combining a common $\alpha_s$ uncertainty together with a PDF uncertainty suitably enlarged in order to keep into account the spread of PDF central values obtained using different PDF sets.

*Procedure A*: This procedure is based on the observation that the change in PDFs and uncertainties when $\alpha_s$ is varied by $\Delta\alpha_s \sim 0.001$ is small, as shown in Fig. 3, and implicitly demonstrated by smallness of the effect it has on $\alpha_s$ and PDF uncertainties, Figs. 10 and 11. Therefore, we can obtain a prediction with a common value of $\alpha_s$ for all groups by simply using the common intermediate value of $\alpha_s = 0.119$ in the computation of the hard cross section Eq. (2), and then using each group's PDFs and full PDF + $\alpha_s$ uncertainties, despite the fact that strictly speaking they correspond to the slightly different values of $\alpha_s$ listed in Eq. (9). Because all predictions are given at the same value of $\alpha_s$, their spread reflects differences in underlying PDFs. Hence, we can take as a conservative estimate of the one-$\sigma$ total PDF + $\alpha_s$ uncertainty on this process the envelope of these predictions, i.e. the band between the highest and the lowest prediction. This procedure would be easiest to implement if all PDF groups were to provide PDFs with a common $\alpha_s$ value and uncertainty. It is still viable provided the central $\alpha_s$ values are not too different, and the $\alpha_s$ uncertainty can be taken as the same or almost the same for all groups.

*Procedure B*: This procedure is based on the observation that in fact the spread of central values of $\alpha_s$ Eq. (9) is essentially the same as the width of the one-$\sigma$ error band Eq. (10). Because the total uncertainty is well approximated by the combination of $\alpha_s$ and PDF uncertainties, this suggests that we can simply replace the $\alpha_s$ uncertainty by the spread of values obtained with the three sets. Hence, a conservative estimate of the one-$\sigma$ total PDF + $\alpha_s$ is

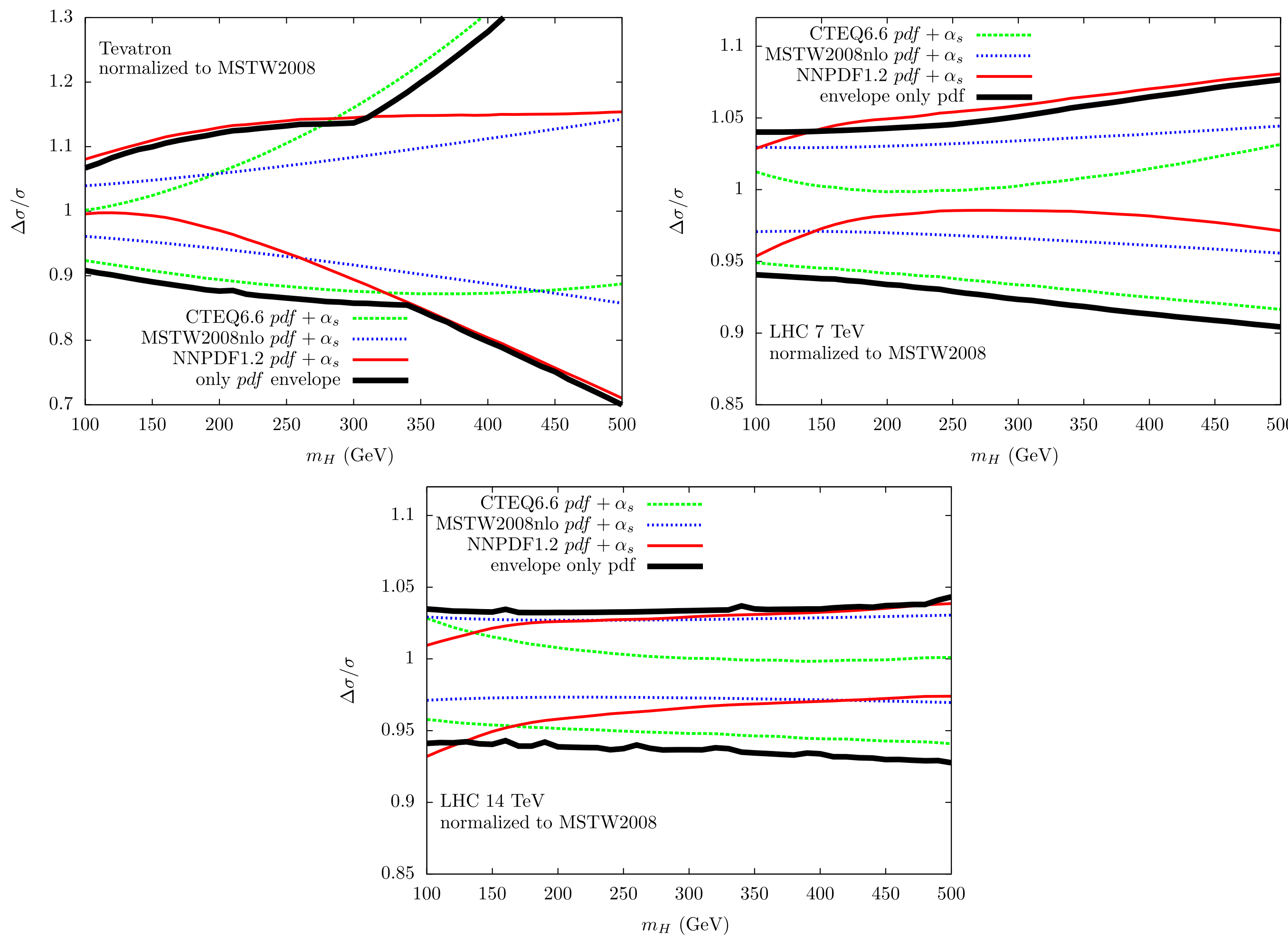


FIG. 13 (color online). The CTEQ, MSTW and NNPDF curves obtained using the common value $\alpha_s = 0.119$ in the cross section Eq. (2), but with the PDF sets and uncertainties corresponding to each group's value of $\alpha_s$ Eq. (9). All curves are normalized to the central MSTW curve obtained in this way. The common prediction can be taken as the envelope of these curves (*Procedure A*). The envelope curve shown (*Procedure B*) is instead the envelope of the CTEQ, MSTW, and NNPDF predictions showed in Fig. 7, obtained including PDF uncertainties only, but with each group's value of $\alpha_s$ used both in the PDFs and cross section, also normalized as the other curves.

obtained by taking the envelope of the PDF-only uncertainty bands obtained using each of the three sets, each at its preferred value of $\alpha_s$ Eq. (9), i.e. the envelope of the bands shown in Fig. 7.

These two conservative estimates are shown in Fig. 13, where we display the uncertainty bands obtained from the three MSTW, CTEQ, and NNPDF sets whose envelope corresponds to the first method, as well as the envelope of the bands of Fig. 7, corresponding to the second method. The results turn out to be in near-perfect agreement, and we can take them as a conservative estimate of the PDF + $\alpha_s$ uncertainty. Note that if any of the three sets were discarded, the prediction would change in a not insignificant way.

Typical uncertainties are, for light Higgs, of order of 10% at the Tevatron and 5% at the LHC. Very large uncertainties are only found for very heavy Higgs at the Tevatron, which is sensitive to the poorly known large $x$ gluon. As a central prediction one may take the midpoint between the upper and lower bands: in practice, this turns out to be extremely close to the MSTW08 prediction found adopting the previous method, i.e. using the MSTW08 PDFs but with $\alpha_s = 0.119$ in the matrix element.

These results for the combined PDF + $\alpha_s$ uncertainties should be relevant for Higgs searches both at the Tevatron and at the LHC. For instance, the latest combined Tevatron analysis on Higgs production via gluon-fusion [22], which excludes a SM Higgs in the mass range 162–166 GeV at 95% C.L., quotes a 11% systematic uncertainty from PDF uncertainties and higher order variations. It would be interesting to reassess the above exclusion limits if the combined PDF + $\alpha_s$ uncertainties were estimated as discussed in this work.

## VII. CONCLUSIONS

We have presented a systematic study of the impact of PDF and $\alpha_s$ uncertainties in the total NLO cross section for the production of standard model Higgs in gluon-fusion. Whereas a full estimate of the uncertainty on this process would also require a discussion of other sources of uncertainty, such as electroweak corrections and the uncertainties related to higher order QCD corrections (NNLO, soft gluon resummation, etc.), our investigation has focussed on PDF uncertainties, which are likely to be dominant for many or most LHC standard candles, and the $\alpha_s$ uncertainty which is tangled with them. The process considered here is one for which these uncertainties are especially large, and thus it provides a useful test case.

Our main findings can be summarized as follows:

(i) Parton distributions are correlated to the value of $\alpha_s$ in a way which is visible, but of moderate significance. In particular, if $\alpha_s$ is varied within a reasonable range, not much larger than the current global uncertainty, uncertainties due to PDFs and the variation of $\alpha_s$ can be considered to good approximation independent and the total uncertainty can be found adding them in quadrature.

(ii) The gluon luminosities determined from MSTW08, CTEQ6.6, and NNPDF1.2 agree to one $\sigma$ in the sense that their uncertainty bands always overlap (though just so for light Higgs at the Tevatron). As a consequence, the Higgs cross sections determined using these PDF sets agree provided only the same value of $\alpha_s$ is used in the computation of the hard cross section. The spread of central values between sets is of the order of the PDF uncertainty.

(iii) The PDF uncertainties determined using these sets are in reasonable agreement and always differ by a factor less than two, while being affected by an uncertainty which is likely to be about half their size. The $\alpha_s$ uncertainties are essentially independent of the PDF set, and provide more than half of the combined uncertainty. The combined uncertainties determined using the sets under investigation are thus in good agreement with each other.

(iv) A conservative estimate of the total uncertainty can be obtained from the envelope of the PDF + $\alpha_s$ uncertainties obtained from each set, all evaluated with a common central $\alpha_s$ value. Equivalently, it can be obtained from the envelope of the PDF-only uncertainties of sets evaluated each at different value of $\alpha_s$, within a range of values which covers the accepted $\alpha_s$ uncertainty.

(v) A typical conservative PDF + $\alpha_s$ uncertainty is, for light Higgs, of order 10% at the Tevatron and 5% at the LHC. This is at most a factor two larger than the PDF + $\alpha_s$ uncertainty obtained using each individual parton set. Exclusion of any of the three sets considered here would lead to a total uncertainty which is rather closer to that of individual parton sets.

Further improvements in accuracy could be obtained by accurate benchmarking and cross-checking of PDF determinations in order to isolate and understand the origin of existing disagreements. However, the overall agreement of existing sets appear to be satisfactory even for this worst case scenario.

## ACKNOWLEDGMENTS

We thank all the members of the NNPDF collaboration, which has developed the PDF fitting methodology and code which has been used to produce the Monte Carlo varying-$\alpha_s$ PDF sets used in this study. S. F. thanks the members of the PDF4LHC workshop for various discussions on PDF uncertainties and their impact on LHC observables, in particular, Joey Huston and Robert Thorne. This work was partly supported by the European network HEPTOOLS under Contract No. MRTN-CT-2006-035505.

*Note added.*—As this paper was being finalized, a study [23] of uncertainties on Higgs production has appeared.

This paper presents detailed investigations of uncertainties which are not being discussed by us, specifically electroweak and scale (higher order QCD) uncertainties, while it addresses only marginally the issue on which we have concentrated, namely, the interplay of $\alpha_s$ and PDF uncertainties. In this paper the assessment of the fraction of uncertainty due to PDFs and $\alpha_s$ at the Tevatron is sizably larger than our own, essentially due to the fact that the uncertainty is inflated to also accommodate results found using the ABKM PDFs of Ref. [24], which give a significantly lower cross section than found using the CTEQ, MSTW, or NNPDF sets. This is likely to be partly due to the fact that ABKM has a low NLO central value of $\alpha_s = 0.1129$. However, the dependence of ABKM results on the choice of $\alpha_s$ cannot be easily assessed because ABKM PDFs and uncertainties are not provided for $\alpha_s$ fixed as an external parameter and then varied, rather, they are only given with $\alpha_s$ treated as a parameter in the fit.


[1] H. M. Georgi, S. L. Glashow, M. E. Machacek, and D. V. Nanopoulos, Phys. Rev. Lett. **40**, 692 (1978).

[2] S. Dawson, Nucl. Phys. **B359**, 283 (1991).A. Djouadi, M. Spira, and P. M. Zerwas, Phys. Lett. B **264**, 440 (1991).

[3] M. Spira, A. Djouadi, D. Graudenz, and P. M. Zerwas, Nucl. Phys. **B453**, 17 (1995).R. Harlander and P. Kant, J. High Energy Phys. 12 (2005) 015.

[4] M. Dittmar *et al.*, arXiv:hep-ph/0511119.

[5] M. Dittmar *et al.*, arXiv:0901.2504.

[6] C. Amsler *et al.* (Particle Data Group), Phys. Lett. B **667**, 1 (2008).

[7] S. Bethke, Eur. Phys. J. C **64**, 689 (2009).

[8] P. M. Nadolsky *et al.*, Phys. Rev. D **78**, 013004 (2008).

[9] A. D. Martin, W. J. Stirling, R. S. Thorne, and G. Watt, Eur. Phys. J. C **63**, 189 (2009).

[10] R. D. Ball *et al.* (NNPDF Collaboration), Nucl. Phys. **B809**, 1 (2009); **B816**, 293(E) (2009).

[11] R. D. Ball *et al.* (The NNPDF Collaboration), Nucl. Phys. **B823**, 195 (2009).

[12] A. D. Martin, W. J. Stirling, R. S. Thorne, and G. Watt, Eur. Phys. J. C **64**, 653 (2009).

[13] E. Mariani, Undergraduate thesis, Milan University, 2009.

[14] R. V. Harlander, Phys. Lett. B **492**, 74 (2000).S. Catani, D. de Florian, and M. Grazzini, J. High Energy Phys. 05 (2001) 025.R. V. Harlander and W. B. Kilgore, Phys. Rev. D **64**, 013015 (2001).Phys. Rev. Lett. **88**, 201801 (2002).C. Anastasiou and K. Melnikov, Nucl. Phys. **B646**, 220 (2002).V. Ravindran, J. Smith, and W. L. van Neerven, Nucl. Phys. **B665**, 325 (2003).

[15] R. Bonciani, G. Degrassi, and A. Vicini, J. High Energy Phys. 11 (2007) 095.U. Aglietti, R. Bonciani, G. Degrassi, and A. Vicini, J. High Energy Phys. 01 (2007) 021.Phys. Lett. B **595**, 432 (2004).Phys. Lett. B**600**, 57 (2004).G. Degrassi and F. Maltoni, Nucl. Phys. **B724**, 183 (2005).Phys. Lett. B **600**, 255 (2004).

[16] ''Review of particle physics'', 2009 partial update, Quantum Chromodynamics review, http://pdg.lbl.gov/2009/reviews/rpp2009-rev-qcd.pdf

[17] J. C. Collins, F. Wilczek, and A. Zee, Phys. Rev. D **18**, 242 (1978).

[18] R. D. Ball *et al.*, arXiv:1003.1241.

[19] R. D. Ball, L. Del Debbio, S. Forte, A. Guffanti, J. I. Latorre, J. Rojo, and M. Ubiali, Nucl. Phys. **B838**, 136 (2010).

[20] M. Krämer, E. Laenen, and M. Spira, Nucl. Phys. **B511**, 523 (1998).

[21] B. Efron, SIAM Rev. **21**, 460 (1979).

[22] T. Aaltonen *et al.* (CDF and D0 Collaborations), Phys. Rev. Lett. **104**, 061802 (2010).

[23] J. Baglio and A. Djouadi, arXiv:1003.4266.

[24] S. Alekhin, J. Blumlein, S. Klein, and S. Moch, Phys. Rev. D **81**, 014032 (2010).